Assessment of the applicability of NO-NO2-O3 photostationary state to long-term measurements at the Hohenpeissenberg GAW Station, Germany

K. Mannschreck, S. Gilge, C. Plass-Duelmer, W. Fricke, H. Berresheim

Atmos. Chem. Phys., 4, 1265–1277, 2004
www.atmos-chem-phys.org/acp/4/1265/
SRef-ID: 1680-7324/acp/2004-4-1265

Atmospheric Chemistry and Physics

Assessment of the applicability of NO-NO_2-O_3 photostationary state to long-term measurements at the Hohenpeissenberg GAW Station, Germany

K. Mannschreck[1], **S. Gilge**[2], **C. Plass-Duelmer**[2], **W. Fricke**[2], **and H. Berresheim**[2]

[1]Umweltforschungsstation Schneefernerhaus, Zugspitze, Germany
[2]Deutscher Wetterdienst, Meteorologisches Observatorium Hohenpeissenberg, Germany

Received: 3 February 2004 – Published in Atmos. Chem. Phys. Discuss.: 7 April 2004
Revised: 30 July 2004 – Accepted: 3 August 2004 – Published: 17 August 2004

Abstract. Continuous measurements of concentrations of reactive gases, radiation, and meteorological parameters are carried out at the Meteorological Observatory Hohenpeissenberg (MOHp) as part of the Global Atmosphere Watch (GAW) Program. NO, NO_2, O_3 and J_{NO2} data from a four-year period (March 1999–December 2002) are evaluated for consistency with photochemical steady state (PSS, Φ=1) conditions. The extent of deviation from PSS reveals a strong dependence on wind direction at the station. Median values of Φ in the south sector are in the range of 2.5–5.7 and show a high variability. In contrast, values for the other directions show a relatively low variability around a median level of 2. When taking into account peroxy radical concentrations (Φ_{ext}=1) PSS was reached in 13–32% of all cases for the years 1999–2002.

The differences in wind sectors can be explained by local effects. It is shown that the height of the sample inlet line, its distance to the forest and the surrounding topography has a strong impact on both the absolute and relative deviations from PSS. Global irradiance and thus, photolysis of NO_2 is reduced within the dense forest. Since the reaction of NO with O_3 is still proceeding under these conditions, increased NO_2/NO ratios are produced locally in air which is transported through the forest and advected to the MOHp site.

Estimates of the peroxy radical concentration (RO_2) inferred from PSS are compared with peroxy radical measurements made at the site in June 2000 during a three-week campaign. The PSS derived RO_2 levels were higher than corresponding measured levels by at least a factor of 2–3. This analysis was made for a wind sector with minimal local effects on PSS. Thus the corresponding Φ median of 2 can be regarded as an upper limit for a deviation from PSS due to chemical reactions, i.e. by peroxy radicals and possible other oxidants converting additional NO to NO_2.

Correspondence to: K. Mannschreck
(k.mannschreck@schneefernerhaus.de)

1 Introduction

NO in the troposphere is converted to NO_2 by reaction with O_3 and – during daytime – photolysed back to NO.

$$NO + O_3 \longrightarrow NO_2 + O_2 \qquad (1)$$
$$k_1 = 1.4 \cdot 10^{-12} \cdot \exp(-1310/T)\mathrm{cm}^3\mathrm{s}^{-1}$$

$$NO_2 + h\nu \longrightarrow NO + O(^3P) \qquad \lambda < 420\,\mathrm{nm} \qquad (2)$$

$$O(^3P) + O_2 + M \longrightarrow O_3 + M \qquad (3)$$

These two processes (1–2) tend to establish an equilibrium on a time scale of 100 seconds (Leighton, 1961), known as the Photostationary State (PSS), which can be described as

$$\frac{[NO_2]}{[NO]} = \frac{k_1\,[O_3]}{J_{NO_2}} \qquad (4)$$

The Photostationary State parameter Φ is defined as:

$$\Phi = \frac{J_{NO_2} \cdot [NO_2]}{k_1\,[O_3]\,[NO]} \qquad (5)$$

where J_{NO_2} is the photolysis rate of NO_2. The value of k_1 in (1) is taken from Atkinson et al. (2002).

Reactions (1–3) determine a quasi-constant PSS ozone level which mainly depends on the NO_2 photolysis frequency. This represents a null cycle in which no additional ozone is produced. Φ is equal to 1 when other reactions converting NO to NO_2 and local emissions of either compound

are negligible. However, these cases are rare and are limited to very polluted conditions. Under clean or moderately polluted conditions particularly peroxy radicals may contribute to additional NO to NO_2 transformation thereby increasing ambient ozone levels beyond PSS:

$$HO_2 + NO \longrightarrow NO_2 + HO \quad (6)$$

$$RO_2 + NO \longrightarrow NO_2 + RO \quad (7)$$

R represents any organic functional group, the simplest being CH_3. In the following the sum of HO_2 and all organic peroxy radical species is defined as RO_2.

At high NO_x (=NO+NO_2) levels significant concentrations of peroxy radicals are not established due to efficient scavenging of OH – the precursor of RO_2 – by NO_2 producing HNO_3 and increased loss of RO_2 by reaction with NO. However, in low-NO_x environments peroxy radicals gain importance and can perturb the PSS. In this case Φ becomes greater than unity which is found over most parts of the troposphere (e.g. Ridley, 1992; Parrish, 1986).

However, several field studies which included measurements of peroxy radicals in addition to NO, NO_2, J_{NO_2} and O_3 showed that measured peroxy radical concentrations were still too low to explain the observed deviations from PSS (e.g. Cantrell et al., 1993; Davis et al., 1993; Hauglustaine et al., 1996; Volz-Thomas et al., 2003; Handisides et al., 2003). Some authors have speculated that an as yet unidentified oxidant XO might have contributed to additional conversion of NO to NO_2 (Parrish et al., 1986; Carpenter et al., 1998; Volz-Thomas, 2003). Assuming important contributions from both an unknown oxidant and the measured peroxy radicals, corresponding steady state conditions can be described by the extended parameter Φ_{ext}:

$$\Phi_{ext} = \frac{J_{NO_2} \cdot [NO_2]}{k_1 [O_3][NO] + k_{6-7}[RO_2][NO] + k_{xo}[XO][NO]} \quad (8)$$

Further contributions to deviations from PSS may result from:

- Local NO_2 sources near the measurement site
- Local NO or O_3 sinks near the measurement site
- Other non-steady state conditions (e.g. rapid changes in J_{NO_2}, O_3...)
- Measurement errors

Since the mid-1990's continuous long-term measurements of a broad range of important tropospheric constituents and physical parameters (e.g. O_3, NO, NO_2, NO_y, $J(O^1D)$, $J(NO_2)$, irradiance) have been conducted at the German Weather Service's (DWD) Meteorological Observatory Hohenpeissenberg (MOHp) as part of the Global Atmosphere Watch program (GAW) of the World Meteorological Organization (WMO). Measurements from March 1999 to December 2002 are evaluated in this study to examine the validity and frequency of occurrence of NO-NO_2-O_3 photostationary state. Due to construction of a new GAW building at the site during 1999 and 2000 the GAW observation platform was housed in a preliminary building during this time. This building was located relatively close to the forest. Accordingly, enhanced local influences on in situ levels of reactive compounds such as NO or NO_2 were to be expected, since it was assumed that the close vicinity of this building to the forest causes a heterogeneity of advected air masses. If the history of an air mass is not known, air chemical investigations can easily be misinterpreted. In order to characterise these conditions in more detail we have now evaluated these measurements with respect to PSS together with 2001–2002 measurements from the new building. The data are systematically analysed by statistical means. This includes a classification by wind direction as well as using results from previous campaign measurements of peroxy radical concentrations at MOHp (Handisides et al., 2003).

2 Experimental

2.1 Measurement Site

The Meteorological Observatory Hohenpeissenberg (MOHp) of the German Weather Service is located approximately 40 km north of the Alps at 985 m a.s.l. (47°48′ N, 11°01′ E) at the top of a solitary hill which rises about 300–400 m above the surrounding area. Since 1994 the station has been operated (complementary with the High Alpine Environmental Research Station Schneefernerhaus) as one of the present 22 WMO Global Atmosphere Watch Stations.

Generally, the site is affected by relatively clean air masses (yearly average of NO_x is below 3.5 ppb), however, maximum values can sometimes reach 12–14 ppb, particularly during stagnant inversion conditions in winter when the site is within the boundary layer.

The site is surrounded by forests (70%, mostly coniferous) and agricultural pastures (30%). The distance to the nearest urban and major industrial areas (e.g. Munich) is about 80 km. In the south sector air masses are predominantly advected from the Alps region at relatively high wind speeds and trace gas concentrations in this sector are relatively low. Possible anthropogenic sources which could influence trace gas concentrations are rural road traffic and small towns (4000–12 000 inhabitants) approximately 5–8 km from the site to the southwest. Air masses from the other directions on average have lower wind speeds and show somewhat higher concentrations of trace gases. Specifically, air from the northeast shows a higher level of pollution due to emissions from a small town at 10 km (20 000 inhabitants) and the city of Munich (1 million inhabitants) at 80 km.

During 1999 and 2000 the instruments for the trace gas measurements were operated in a preliminary building

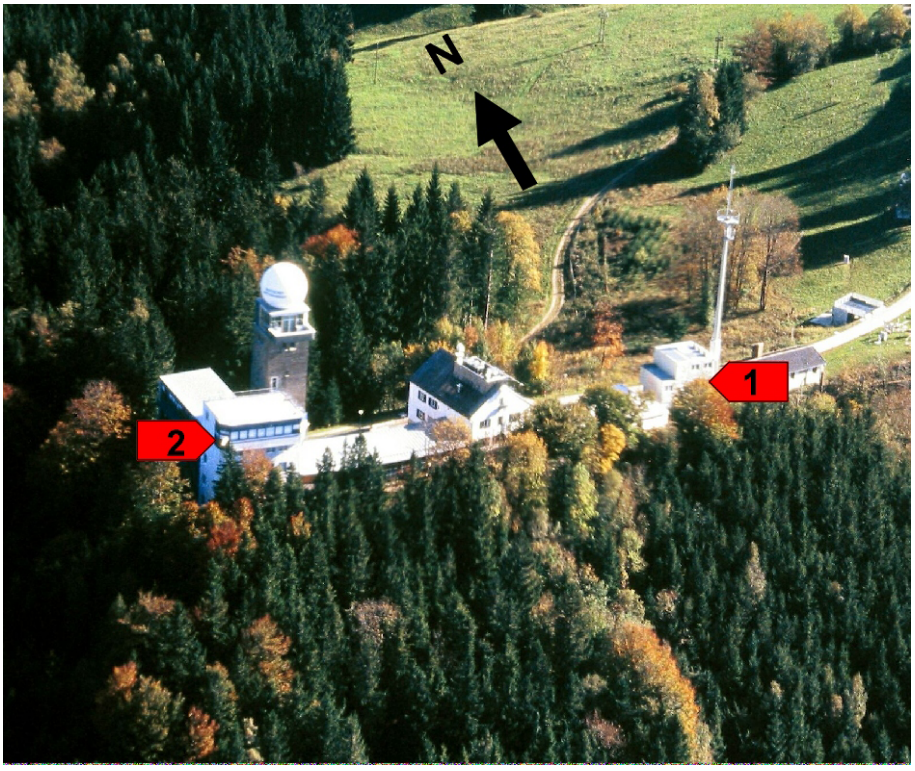

Fig. 1. The Meteorological Observatory Hohenpeissenberg. Measurements were performed in the preliminary building (position 1) during 1999 and 2000, and in the new building (position 2) during 2001 and 2002.

(position 1, Fig. 1) with the air inlets at approximately 10 m above ground level. This corresponded to some 2 m below the canopy tops of trees and about 3 m of horizontal distance to the nearest trees of the forest located in the sector between 105° and 290°. North of the building (290°–70°) the distance to the trees was about 100 m. To the east of the building (70°–105°) there are meadows, a parking lot and some houses but no trees.

In April 2001 the instruments were moved to the new GAW building (position 2, Fig. 1) about 100 m further northwest. Sample inlets at the new location are located approx. 15 m above ground. The horizontal distance to the nearby forest in the sector between 115°–135° is approx. 200 m, between 135°–190° approx. 50 m and between 190°–270° approx. 10 m. In the latter case the air inlet is approximately at the canopy height of the trees. The sector between 270°–360° is characterised by a steep slope and the inlet line is well above the canopy height of the trees which are in a distance of at least 10 m in this direction. To the northeast (0°–90°) the forest is about 200 m away, however, partial shading of air parcels flowing along the northwestern edge of the building is possible when air is advected parallel to the ground rather than from aloft. The sector between 90°–115° is free of trees and characterised by meadows and the parking lot.

Temperature, pressure, and humidity were measured at the ground at a horizontal distance of 50 m and 100 m from the provisional and the new building, respectively, and wind measurements were made at the top of a 40 m mast.

2.2 Measurement Program

Based on Eq. (5) an experimental verification of PSS conditions requires simultaneous measurements of NO, NO_2, O_3, J_{NO_2} and ambient temperature (to account for the temperature dependence of k_1). Table 1 summarises the analytical techniques used to determine the individual parameters.

Ozone is measured simultaneously with two UV absorption instruments (Thermo Environmental Instruments Inc., Model TECO 49C and Dasibi), a chemiluminescence-based instrument (UPK, Germany) and a self-built wet chemical method (potassium iodide). According to GAW QA regulations ozone analysers are calibrated at regular time intervals with a transfer standard (TECO 49 PS). In addition, ozone measurements have been validated by audits carried out by the GAW World Calibration Centre for ground-based ozone measurements (EMPA, Switzerland).

Nitrogen oxide species are measured with three analysers and two different chemiluminescence methods. Two analysers are based on chemiluminescence of NO with ozone measured with a chemiluminescence detector, CLD

Table 1. Analytical techniques employed at MOHp. Uncertainty and detection limit refer to a time interval of 10 min.

Parameter	Instrument	Uncertainty ($\pm 1\sigma$)	Detection limit
NO	CLD 770AL (EcoPhysics)	5.3% (min. 15 ppt)	15 ppt
NO_2	CLD 770AL (EcoPhysics) Photolytic converter (PLC, EcoPhysics)	5.7% (min. 30 ppt)	20 ppt
	Luminox LMA-3 Scintrex Unisearch S.A.	8% (min. 50 ppt)	50 ppt
NO_y	CLD 770AL (EcoPhysics) Gold converter	10.3% (min. 50 ppt)	50 ppt
O_3	TECO 49C (Thermo Env. Instr.)	4.5%	1 ppb
CO	TECO 48S (Thermo Env. Instr.)	5%	10 ppb
J_{NO_2}	Filterradiometer, Meteorologie Consult GmbH, Germany	14%	$<1{\cdot}10^{-5}\,s^{-1}$

(ECO-Physics CLD 770 AL ppt). One of these is operated in combination with a photolytic converter, PLC (ECO-Physics PLC 760) which converts NO_2 to NO specifically and the other with a gold converter (gold tube at 300°C in the presence of 0.1% CO) which converts NO_y to NO.

The second method makes use of the chemiluminescence of NO_2 reacting with luminol (Scintrex Unisearch LMA-3) which is also detected with a CLD. NO is oxidised quantitatively to NO_2 by leading the gas flow over a CrO_3-filter. The luminol instrument serves as backup and for quality control. For NO_2 both methods agree better than 1%.

The NO_x instruments are routinely calibrated every second day with a known flow of calibration gas (5 and 10 ppm NO in N_2, Messer, Germany) which is dynamically diluted to atmospheric concentration ranges. The conversion efficiencies of the PLC and the gold converter for NO_2 are determined by measurements of NO_2 produced by gas phase titration of the NO standard with ozone. In addition, the NO_y measurements are checked with a HNO_3 permeation source (self-built). Deviations between two calibrations are typically well below 2%.

For quality control several informal intercomparisons with other instruments under calibration and ambient air conditions were carried out in the last years, the last one in August 2002. Under ambient air conditions (ranges: lower than detection limit up to 1.3 ppb for NO, 0.4–4.3 ppb for NO_2, 2.3–4.5 ppb for NO_y) the deviations between the two systems (MOHp and German Aerospace Centre, DLR Oberpfaffenhofen) were well below 5% in the case of NO, below 1% for NO_2 and below 5% for NO_y at correlation coefficients of r=0.96, 0.98 and 0.90 respectively. Thus, the deviations are smaller than the overall measurement uncertainties (MOHp/DLR) of 5.3%/5.9%, 5.7%/7.5% and 10.3%/8.6% for NO, NO_2 and NO_y respectively.

CO is measured with a Thermo Environmental Instruments Analysator (48 S) which uses the measurement principle of the non dispersive infrared absorption spectroscopy (NDIR) accompanied with gas filter correlation (GFC). Due to the strong interference with water vapor, which can considerably influence the measuring signal at remote or rural stations, this commercial instrument was further modified at MOHp to measure carbon monoxide free of H_2O interference (Parrish et al., 1994). The ambient air is first led directly into the analyser for ten minutes. In a second step the ambient air is led over a palladium catalyst heated to 150°C where CO is oxidised quantitatively to CO_2 before being analysed. The difference between these two cycles gives an interference free signal of ambient CO mixing ratios. The detection limit of this set up is about 10 ppb.

J_{NO_2} is quantified by measuring the UV actinic flux with two (up- and downward) 2π steradian filter radiometers. The calibration is based on measurements versus an actinic spectral radiometer by Research Centre Jülich (B. Bohn, personal communication) in 2001, with a resulting accuracy of our filter radiometers of 13% each. The J_{NO_2} obtained by the actinic spectral radiometer had been compared with chemical actinometry before (Kraus et al., 2000) and an overall accuracy of 10% had been determined (Kraus et al., 2000). For calculation of J_{NO_2} from spectral radiometer data, the NO_2 absorption cross section determined by Merienne et al. (1995) and the quantum yields determined by Troe (2000) were used. For the time period considered (1999–2002), no change in the sensitivity of the filter radiometer was detected. This is based on three independent approaches: (1) The radiometers were calibrated in 1997 and 2001 against a "master" filter radiometer by the manufacturer with insignificant sensitivity changes of less than 3%. (2) For the period 1999 to 2002, the filter radiometer results obtained for clear sky

Table 2. Number of 10 min mean values for each year. Second column refers to the number of all NO_x values, third column to all NO_x values for which $J_{NO_2} \geq 6 \cdot 10^{-3}\,s^{-1}$, and last column to number of data for which Φ values were calculated, i.e. simultaneous measurements of NO_2, NO, O_3, J_{NO_2} and T were available and $J_{NO_2} \geq 6 \cdot 10^{-3}\,s^{-1}$.

year	number of all data	number of data with $J_{NO_2} \geq 6 \cdot 10^{-3}\,s^{-1}$	number of Φ values
1999	36408	6200	4467
2000	46434	6144	5376
2001	46447	5431	4970
2002	48313	6973	6778

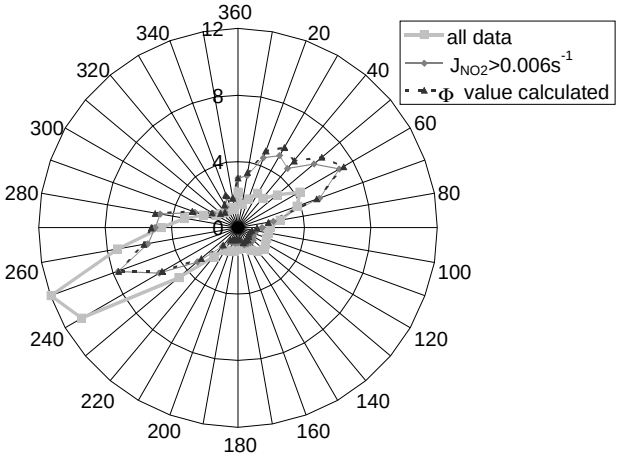

Fig. 2. Average relative frequency of wind direction in % for the period March 1999–Dec 2002. Bold grey line: all data, thin grey line: all data with $J_{NO_2} \geq 6 \cdot 10^{-3}\,s^{-1}$, dotted black line: all data for which Φ was calculated, i.e. simultaneous measurements of NO_2, NO, O_3, J_{NO_2} and T were available and $J_{NO_2} \geq 6 \cdot 10^{-3}\,s^{-1}$.

conditions were checked for sensitivity changes by comparison with J_{NO_2} values calculated by the model STAR (System for Transfer of Atmospheric Radiation, Schwander et al., 2001). The radiometer sensitivities showed small, unsystematic changes by less than 2% from year to year, which is not significant. (3) Using a polynomial fit (2^{nd} order) between J_{NO_2} and the global irradiance, measured J_{NO_2} can be plotted versus fitted J_{NO_2} based on the measured global irradiance. Again, the slope of this linear relation did not change significantly from year to year, over the whole period changes were less than 4%. Thus, our J_{NO_2} data for 1999–2002 at levels above $6 \cdot 10^{-3}\,s^{-1}$ had an overall accuracy of 14% and a precision of better than 2%.

2.3 Data Base

One minute time-resolved data obtained for all meteorological, physical and chemical parameters were averaged to 10 min mean values. Each year of the total period under investigation (March 1999–December 2002) is separately analysed.

Only very sunny periods with $J_{NO_2} \geq 6 \cdot 10^{-3}\,s^{-1}$ were selected to verify photostationary state conditions (according to e.g. Volz-Thomas et al., 2003). Based on 10 min mean NO_x values Table 2 shows the total number of all data available from the above period, the number of all data with $J_{NO_2} \geq 6 \cdot 10^{-3}\,s^{-1}$, and the number of available Φ values, which could be derived from simultaneous measurements of NO_2, NO, O_3, J_{NO_2} and T and discriminated by $J_{NO_2} \geq 6 \cdot 10^{-3}\,s^{-1}$. Figure 2 presents the frequency distribution of the wind direction averaged over the 4 year period. In general, the prevailing wind direction at MOHp is WSW followed by NE. When applying the criterion for J_{NO_2}, the relative amount of data is significantly reduced for the WSW sector and increased for the NE sector so that the relative frequency becomes similar for both sectors.

3 Experimental results

Figure 3 presents the dependence of the mean annual CO and NO_x concentrations on wind direction for daytime clear sky conditions ($J_{NO_2} \geq 6 \cdot 10^{-3}\,s^{-1}$) for each year. CO and NO_x are tracers for anthropogenic pollution mainly originating from road traffic, industrial and domestic combustion processes. The typical atmospheric lifetimes of NO_x and CO with respect to reaction with OH are less than 1 day and 3–4 weeks, respectively. CO has a uniform distribution for all directions with a slight enhancement in the sector 0–100°. NO_x levels are more variable with a minimum in the sector 300°–40°. Note that without J_{NO_2} filtering (i.e. using all available data) the corresponding wind directional plots for NO_x look somewhat different showing a NO_x maximum in the NE direction due to emissions from the urban region of Munich (80 km distance). In this sector the percentage of clear sky data is above average (see Fig. 2). Since the lifetime of NO_x is reduced during periods of high J_{NO_2}, the mean NO_x values are lowered disproportionally when applying the J_{NO_2} filter criterion. The maximum NO_x concentration observed for the clear sky data originate from small towns at a distance of about 10 km.

The dependence of the median values of Φ on wind direction is shown in Fig. 4. Φ was determined as defined in Eq. (5). While during all years Φ is around 2 for the west, north and east sector, the two periods 1999–2000 (preliminary building) and 2001–2002 (new building) show differences in the south sector. During 1999–2000 Φ medians of 3.5–5.7 are found for the sector 130°–260°, and values of 2.5–3.8 for the sector 150°–250° during 2001–2002.

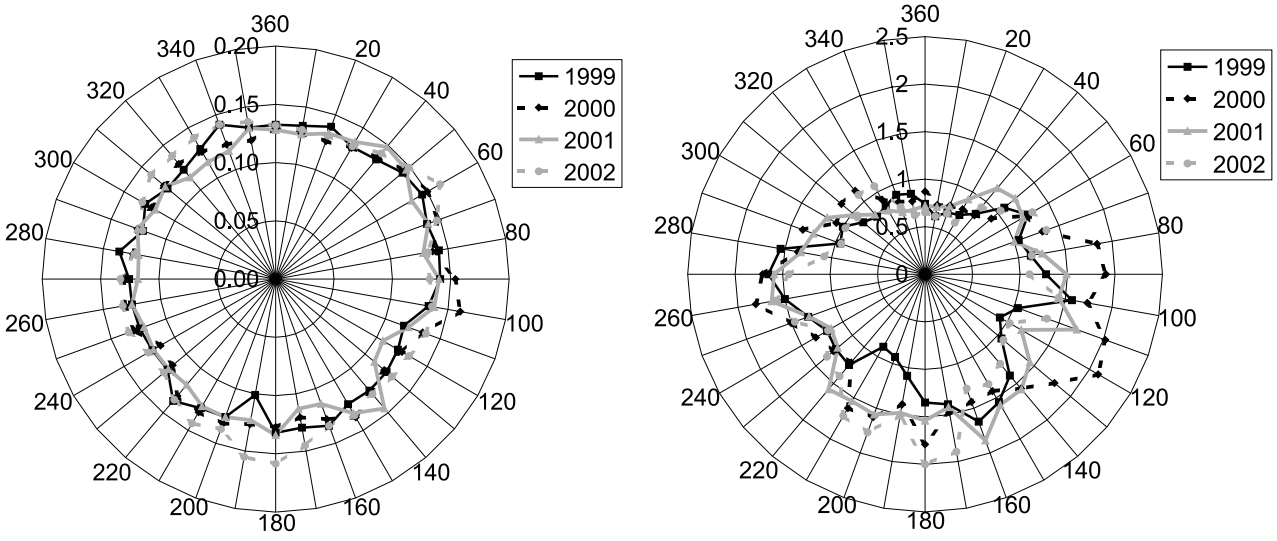

Fig. 3. Dependence of CO (left panel) and NO_x (right panel) levels on wind direction (annual means in units of ppb). Only data with $J_{NO_2} \geq 6 \cdot 10^{-3}\,s^{-1}$ are considered.

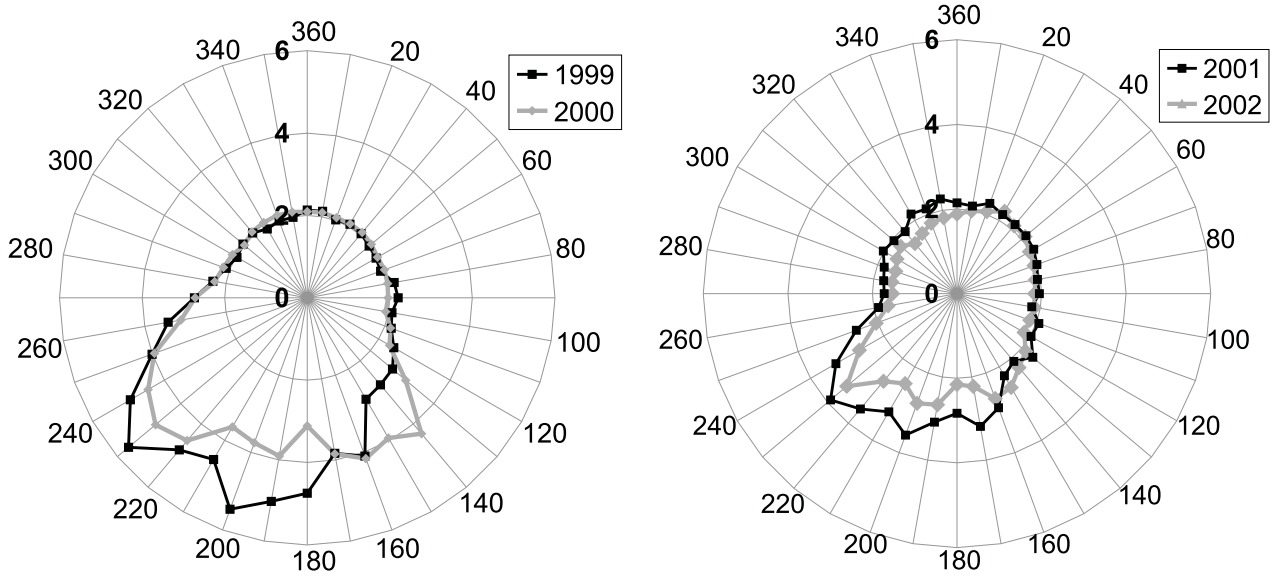

Fig. 4. Dependence of medians of Φ on wind direction for each year. Only data with $J_{NO_2} \geq 6 \cdot 10^{-3}\,s^{-1}$ are considered.

In Fig. 5 a different approach is used to show the deviation from PSS. This approach is based on Φ_{ext} calculated using (8) with [XO]=0 and taking into account a RO_2 mixing ratio which was determined as a function of J_{NO_2}.[1]

The plot presents the frequency distribution of all data with $\Phi_{ext}=1\pm0.2$, i.e. cases in which PSS conditions prevailed . The range of ±0.2 was chosen since the overall uncertainty is 20% as will be discussed in the next section. Based on this approach PSS was reached in 17% and 13% of all cases, respectively during 1999 and 2000. While the highest percentage (approx. 40%) is reached for the east sector (80°–100°), PSS is reached in less than 20% of cases for all other wind directions. During 2001 and 2002 PSS was reached in 22% and 32% of all cases, respectively with a maximum of approx. 60% for northwest.

[1]Measurements of RO_2 and J_{NO_2} during a three-week campaign at MOHp (see next section) were used to derive the dependence of [RO_2] on J_{NO_2}. The two data sets showed a linear correlation in the observed range. Hence, a linear function was used as a first approximation to calculate [RO_2] from measured J_{NO_2}: [RO_2]=3214*J_{NO_2} [s^{-1}]+13 (in units of ppt).

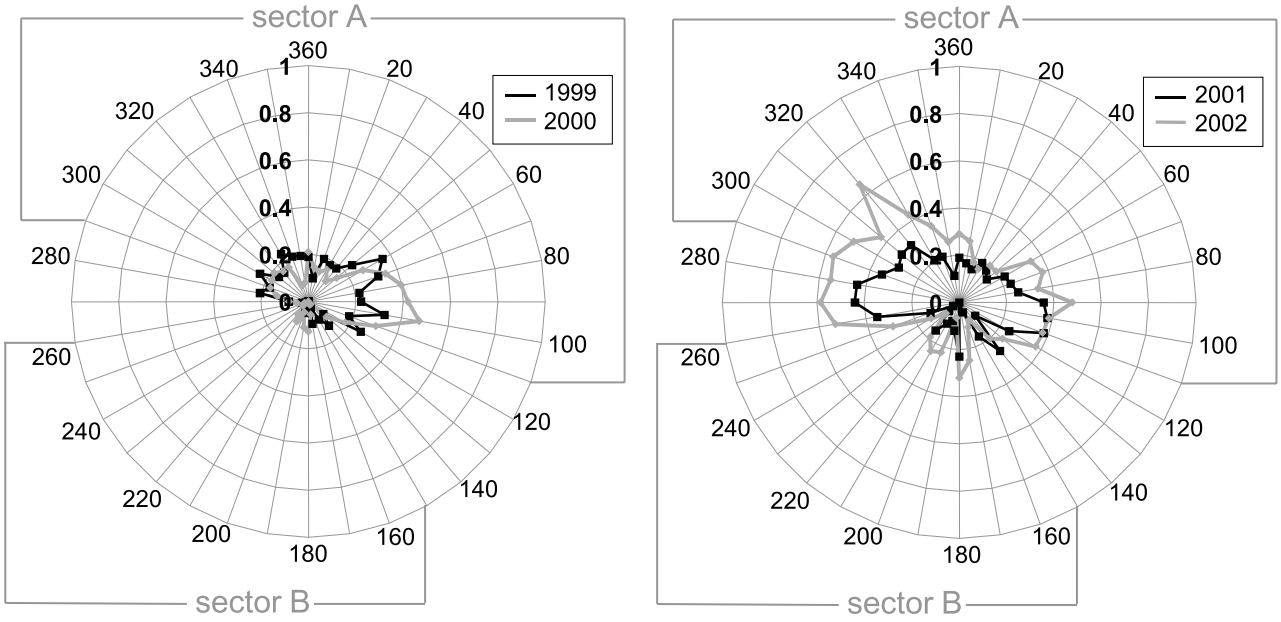

Fig. 5. Frequency distribution of cases (10 min means) for which PSS was established during each year. PSS was considered to be established for Φ_{ext} values between 0.8–1.2. Φ_{ext} was calculated using (8) with [XO]=0 and taking into account a RO_2 concentration which was determined as a function of J_{NO_2} (see footnote 1). Only data with $J_{NO_2} \geq 6 \cdot 10^{-3}\,s^{-1}$ are considered. Sector A (small deviation from PSS) and B (large deviation from PSS) refer to text in next section.

4 Discussion

Our results show that deviations from PSS at MOHp are influenced most by the history of an air parcel which is associated with the wind directions. A secondary but still significant contribution is due to the characteristic differences between the two measurement sites as described earlier.

Published studies based on similar measurement conditions (rural or suburban) report Φ values of 1–3 (Parrish, 1986, Hauglustaine et al., 1996; Volz-Thomas et al., 2003) and 1.8–1.9 (Rohrer, 1998; Ridley et al., 1992). Our results are similar to these data except for the sector 130°–260° during 1999–2000 which exhibits values higher by a factor of 2.

Several previously conducted experiments also included measurements of peroxy radicals which were then compared with PSS theory. These studies included measurements under different levels of pollution: $[NO_x]<0.1$ ppb (Hauglustaine, 1996), NO_x 0.1–1.5 ppb (Cantrell, 1993; Davis, 1993; Frost, 1998; Cantrell 1997) and $NO_x>1.5$ ppb (Volz-Thomas, 2003; Baumann, 2000; Carpenter, 1998). Generally, RO_2 concentrations calculated from assuming PSS were significantly higher than directly measured values. NO_x levels at MOHp are typically in the range of 0.5–3 ppb but can reach higher values especially in winter due to frequently enhanced emissions and sustained inversion layers reaching up to the site. Possible causes which could explain the deviations from PSS observed at MOHp including their differences between individual wind sectors are discussed in the following section.

The overall uncertainty of Φ can be calculated by propagation of errors using the individual uncertainty in each parameter (given in Table 1) from (9).

$$\sigma_\Phi = \sqrt{\sum \left(\sigma_{Y_i}\right)^2 \cdot \left(\frac{\delta \Phi}{\delta Y_i}\right)^2} \tag{9}$$

Generally, for $NO_x>1$ ppb the overall uncertainty is 20% on average and is dominated by the uncertainty of J_{NO_2}. For smaller NO_x mixing ratios the uncertainty resulting from the measurement of NO dominates the overall uncertainty which approaches 60% with decreasing NO_x. Using (9) we have not considered the uncertainty of 5% in both NO and NO_2 arising from the uncertainty in the NO calibration gas as a systematic error which does not contribute to the uncertainty of the ratio.

The differences in Φ values observed between the two periods for each wind sector (Fig. 4) are not significant on a 1σ confidence level. Differences between the sector 130°–260° and the remaining wind directions for 1999–2000 are significant on a 1σ confidence level, differences between the sector 150°–250° and the remaining wind directions for 2001–2002 are not significant. However, note that all results are based on one data series (i.e. same instrument, same calibration

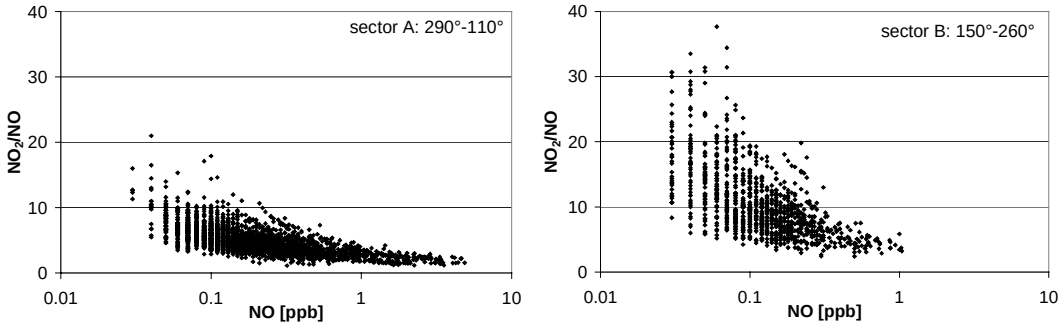

Fig. 6. Dependence of NO_2/NO ratios on the NO mixing ratio during 1999 (10 min means) for the two sectors A and B (see text).

procedures etc.). Therefore, we may assume that measurement errors for one wind direction generally do not have the opposite sign as for the other. Furthermore, in the case of J_{NO_2} the uncertainty is dominated by systematic uncertainties due to actinometry or the assumed absorption cross section and quantum yields. As stated in Sect. 2.2 the precision of J_{NO_2}, a measure which is more meaningful when comparing the two data sets, is better than 2%.

In order to investigate the reasons for the observed differences between the wind directions two sectors are defined according to their level of deviation from PSS: Sector A (small deviation from PSS): 290°–110°; sector B (large deviation from PSS): 150°–260°. These two sectors are chosen as intersections of both periods so that they can be applied for both periods under investigation. Figure 6 compares the NO_2/NO ratios as a function of NO for sectors A and B for 1999 as an example, the plots for the other years are very similar.

In our data the dependence of NO_2/NO on NO corresponds to the dependence of Φ on NO. This variation is in accordance with the current understanding of radical photochemistry (see (6) and (7)). For high NO_x concentrations the levels of peroxy radicals should approach zero, since the sink for RO_2 increases with increasing NO and since OH as a precursor for RO_2 as well as RO species are removed via reaction with NO_2.

For both sectors the variability of NO_2/NO ratios increases with decreasing NO mixing ratios. Generally, high scattering at low NO levels is expected, since the uncertainty in NO measurements close to the detection limit becomes relatively high. For example, when assuming an uncertainty of 50% at 30 ppt NO and NO_2/NO=20, a scatter of $\pm$50% (i.e. NO_2/NO=10–30), as observed for sector B, could be explained by the uncertainty in NO measurements alone. However, this strong variability is not observed for sector A. This indicates firstly, that the uncertainty is somewhat overestimated and secondly, that the strong scatter for sector B at low NO concentrations is at least partly due to the fact that the PSS equilibrium in these cases was not fully established resulting in higher values of NO_2/NO. Here we hypothesise that this deviation from PSS mainly resulted from the fact that the transport time from the point of PSS disturbance (e.g. by a local source of NO_2, or sink of O_3 or NO) to the measurement site was too short to re-establish PSS and/or the NO_2 photolysis over a large area in this sector did not vary as suggested by the J_{NO_2} values measured at the MOHp site.

During 1999 and 2000 the mean NO_2 fraction of NO_x for WSW and NE was 90% and 85%, respectively. A NO_2 source which could disturb the PSS leading to higher values and a high variability must therefore produce a local NO_2 fraction in this range. Possible local NO_2 sources are diesel vehicles. However, typical NO_2/NO_x mixing ratios found in diesel vehicle exhaust are about 13% (Carslaw and Beevers, 2004). Moreover, the traffic density is very low in the vicinity of the site except for occasional tourist traffic about 300 m to the east, and in WSW direction the distance to the only country road is at least 700 m. Hence, we conclude that diesel vehicles cannot be the major cause for the observed deviations from PSS.

On the other hand, a possible sink for ozone is dry deposition, e.g. within the forest. Due to the close vicinity to the forest and the steep slope in southerly direction of the preliminary building air masses advected from this sector are more likely to be transported through the forest than air masses from other directions. If depositional loss of ozone is significant during transport through the forest this would lead to increased Φ values for the south sector. The significance of this potential PSS deviation was investigated by comparing the ozone measurements taken from the provisional building with those measured simultaneously on top of a nearby tower (height of inlet line: 50 m above ground, 30 m above canopy height) during 1999 and 2000. It is assumed that air masses reaching the top of the tower have been – to a higher percentage – transported above the forest canopy rather than being "filtered" through the forest in contrast to air masses reaching the lower sampling point of the provisional building. The comparison between both measurement positions showed no differences in ozone levels within the

measurement uncertainty of 5%. This shows that dry deposition of ozone was not large enough to explain any of the observed differences in Φ.

Another reason could be possible contributions from biogenic hydrocarbons and aerosols from forest sources which might provide sinks of NO and O_3. However, measured mixing ratios of monoterpenes which are most reactive with ozone, were always well below 1 ppb. The integrated turnover rate in reactions with ozone of all biogenic hydrocarbons was calculated to be 0.2 ppb/h on average at noon time in summer months. Thus, reactions of biogenic hydrocarbons with O_3 cannot provide a significant sink for ozone. Moreover, the deviations from PSS do not show a pronounced seasonal variation. This, however, should be the case if any interactions of biogenic hydrocarbons and aerosols with NO and O_3 would have a significant impact on PSS.

A possible explanation for the observed scattering in the NO_2/NO ratio for sector B would be a source of NO_x with a variable emission flux and close distance to the measurement site so that time is too short for PSS to be established. Figure 7 shows the dependence of NO_x on wind direction on the basis of 5, 10, 20, 50, 80, 90 and 95 percentiles. Only the plot for the year 2000 is presented as an example, the other years show similar results. A variable source should show a distribution which is broader in the respective sector. However, this is not the case, no such signal can be detected.

Figure 8 shows that not only the median values of Φ are relatively higher in wind sector B but that also the differences between the various percentiles are larger (note the logarithmic scale). Only the plots for 2000 and 2002 are shown as examples. For 2000 the deviation of the 5 and 95 percentiles from the median for sector B are −51% and +113% of the median, respectively and −34% and +53% of the median for sector A. For 2002 the deviations are −44% and +107% for sector B and −30% and +55% for sector A.

The strong dependence of the NO_2/NO ratio, the Φ value and the variation of Φ on the wind direction, as well as the fact that similar results are found for the two periods respectively, i.e. preliminary building and new building, indicates that local effect at the two sites have a substantial influence on the establishment of PSS. Apart from the height of the inlet line, the two sites differ in their direct surrounding in terms of topography and natural cover. As described in Sect. 2.1 in deteail, advection of air masses to the preliminary building from the east and – to less extent – from the north is relatively unobstructed compared to southerly and westerly direction. In the case of the new building free advection should be favoured from northwest direction compared to the other sectors.

Synthesis of Data Interpretation

Our explanation for the observed influence of the station's surrounding on PSS is as follows: NO_2/NO ratios of

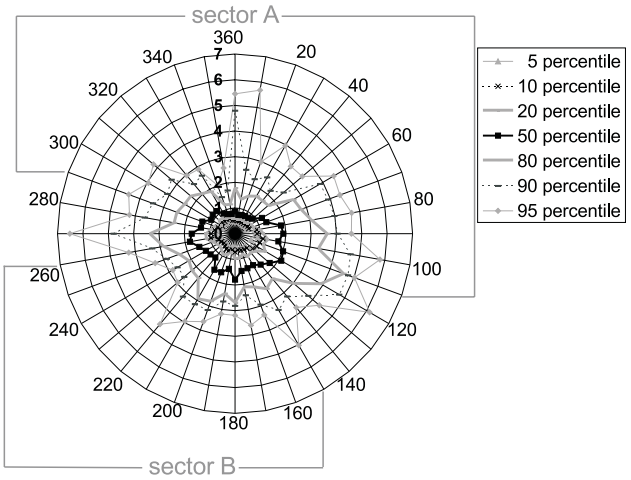

Fig. 7. Dependence of NO_x level on wind direction for 2000. 5, 10, 20, 50, 80, 90 and 95 percentiles are shown.

air masses which are transported from within the forest will increase within the forest (1 km pathway) due to reaction of NO with O_3. At the same time, the major source of NO, namely photolysis of NO_2, is substantially reduced due to reduced light penetration within the denser forest area. For an air parcel arriving from the forest the time is too short (less than 2 s for the mean wind speed of 6 m/s) to establish steady state conditions before being analysed. The measured air is most likely a mixture of air parcels from within the forest and aloft, the share being dependent on the surrounding orography, boundary layer structure and thermal convection. On the other hand free advection enables photolysis of NO_2 leading to a higher percentage of PSS cases. It can be concluded that local factors such as vegetation, topography, relative position of the inlet line and advection patterns of air masses have a substantial influence on PSS and could obscure chemical mechanisms. Since the forest is largely coniferous little seasonal variation is expected in the observed effects. Similar factors may have influenced previous campaign studies in various environments and should be considered in future field experiments. This result of the present study is of general importance and not restricted to the specific environment of MOHp.

The reason for the extremely low frequency of PSS conditions in the northern direction for the preliminary building and north easterly direction for the new building is not yet clear at this time, since for both sites the forest in this direction is not closer than to the east. However, it is assumed that the topography – namely the relatively smooth slope to the north and northeast – influences the wind flow streamlines leading to a higher percentage of air flow through and thus, a longer residence time in the forest.

From 18 June until 6 July 2000, measurements of RO_2 using a chemical amplifier technique were performed at the site (Handisides et al., 2003). Daytime maximum RO_2 levels were 50–70 ppt for clear sky conditions, the accuracy was

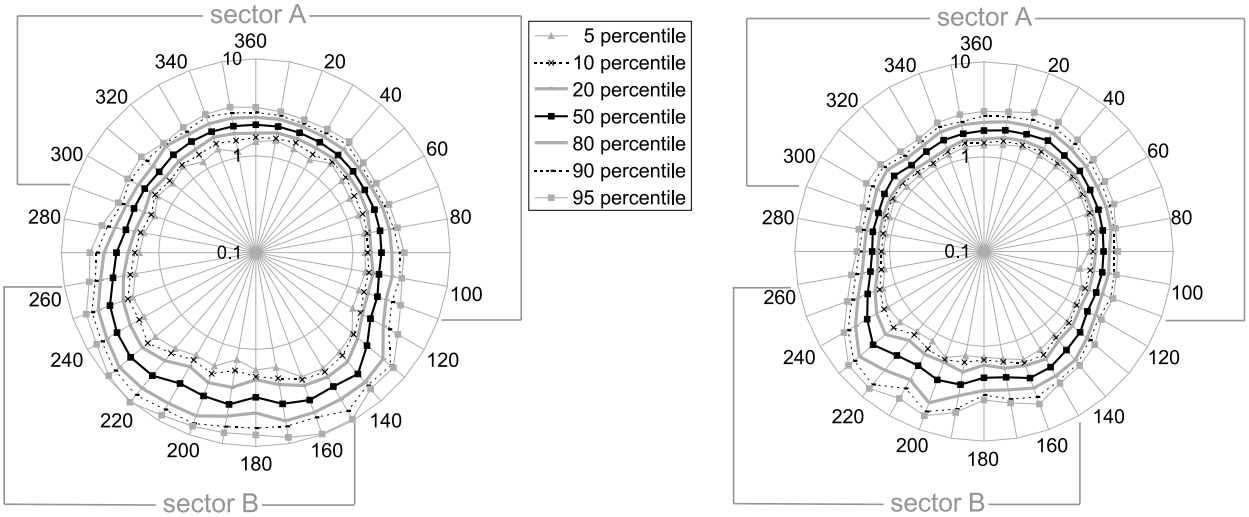

Fig. 8. Dependence of Φ on wind direction for 2000 (left panel) and 2002 (right panel). Φ was calculated using Eq. (5). 5, 10, 20, 50, 80, 90 and 95 percentiles are shown. The radial axis is a logarithmic scale.

better than 60%. The results from these measurements are used here to investigate how large deviations from PSS are under conditions with minimum interference by local effects. As taken from Fig. 8 sector 0°–80° exhibits the smallest median values of Φ and the lowest variation in Φ during 2000. According to the earlier discussion it is assumed that for this sector potential impacts on PSS from forest "filtration" were minimal. Therefore, data from this sector are used to compare measured and PSS derived peroxy radical mixing ratios. PSS derived RO_2 levels were determined from

$$RO_2 = \frac{J_{NO_2} \cdot [NO_2] - [O_3] \cdot [NO] \cdot k_1}{[NO] \cdot k_{6-7}} \quad (10)$$

k_{6-7} is the average rate coefficient for the reaction of the different peroxy radicals with NO. Handisides et al. (2003) assumed that 50% of RO_2 radicals are HO_2 and the main part of organic peroxy radicals is CH_3O_2. Therefore, k_{6-7} was calculated as the average of the rate coefficients of reactions with HO_2 and CH_3O_2 as given by Atkinson et al. (2002). The assumptions concerning the partitioning of RO_2 were discussed by Handisides et al. (2003). It was found that the average rate constant is only weakly sensitive towards assuming other partitionings. For example, assuming a 2:1 ratio between the levels of organic peroxides and HO_2, and assuming that 50% of the organic peroxides are organics with longer R chains than methyl, the average rate constant would still only change by a few percent.

The overall diurnal RO_2 variation measured during this period is shown in Fig. 9. The error bars refer to the 1σ standard deviation of the 10 min mean values. Clearly, PSS derived RO_2 values are systematically higher than measured RO_2 values by a factor of 2–3. They also show a higher variability. The uncertainty in PSS derived RO_2 concentrations is high since they are calculated from the difference between two terms of similar magnitude. When using the PSS derived NO_2/NO ratio with directly measured NO_2/NO ratios for comparison the uncertainty is reduced (Cantrell et al., 1997). Rearranging (10) to solve for NO_2/NO yields:

$$\frac{[NO_2]}{[NO]} = \frac{1}{J_{NO_2}} (k_{6-7} \cdot [RO_2] + k_1 \cdot [O_3]) \quad (11)$$

The uncertainties for the measured and PSS derived NO_2/NO ratios were calculated by propagation of errors. Average uncertainties of 17% for measured and 20% for PSS derived NO_2/NO ratios were determined.

The deviations of PSS derived NO_2/NO ratios from measured ratios are plotted in Fig. 10 against NO. The dotted line refers to the mean uncertainty of the parameter calculated for NO classes of 0.02 ppb intervals from the square root of the sum of uncertainties of measured and PSS derived ratios. Only 35% of all data points lie within this uncertainty range. For 62% of the data points the deviation is higher and so cannot be explained by statistical errors. For the remaining 5 data points the PSS derived NO_2/NO ratio is higher than the measured one.

Using the k_1 value recommended by the NASA panel ($3.0 \cdot 10^{-12} \cdot \exp(-1500/T)$, Sander et al., 2003) yields a slightly better agreement between measured and PSS derived data compared with the Atkinson et al. (2002) value. The mean deviation as calculated for Fig. 10 is reduced from 27% to 23%.

As discussed above local effects should be small for the selected wind sector and therefore, the corresponding Φ median value of 2 can be regarded as an upper limit for a deviation from PSS due to chemical factors. Since the measured RO_2 levels are too low by a factor of 2–3 to explain this deviation, it is concluded that unknown oxidation processes must be important.

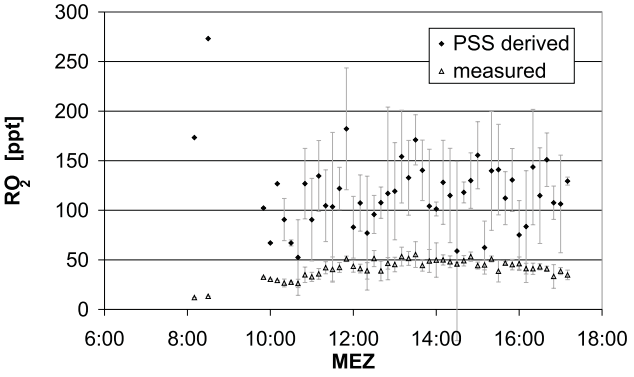

Fig. 9. Mean diurnal variation of measured and PSS derived RO_2-radicals for the sector 0–80° and the time period of 18.6.–6.7.2000. Error bars refer to the 1σ-standard deviation.

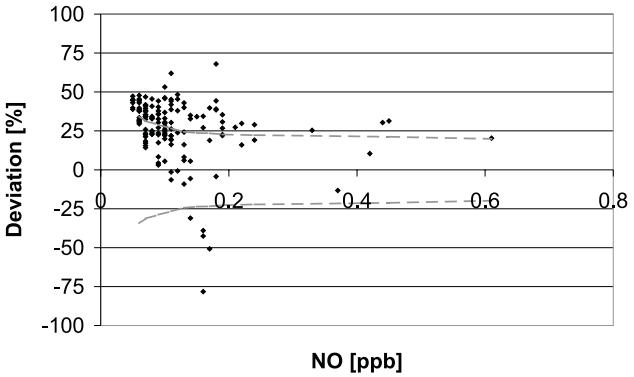

Fig. 10. Deviations of PSS derived NO_2/NO ratios from measured ones as a function of [NO] for the same time period and wind sector as in Fig. 9. The dotted line refers to the mean uncertainty of the parameter calculated for NO classes of 0.02 ppb intervals from the square root of the sum of uncertainties of measured and PSS derived ratios.

Major contributions from halogen or halogen oxide radicals which could efficiently convert NO to NO_2 are not likely since mixing ratios would have to be in the 30 ppt range to explain the observed deviations from PSS in conjunction with the measured RO_2. However, concentrations over 5 ppt are unlikely to occur in rural continental air (Hausmann and Platt, 1994). If there is an unknown oxidant which causes the deviations, it is difficult to characterise its nature and to assess its importance without direct measurements. Correlations of Φ with other species which are measured on a routine basis at MOHp (SO_2, ROOH, number of particles, surface of particles) did not show any relation which could explain this phenomenon. Volz-Thomas et al. (2003) addressed the question if an unknown oxidation process may lead to a net production of ozone or, alternatively, if an unknown species X is formed with simultaneous consumption of ozone. From ozone budget calculations for a city plume based on airborne measurements at different points of the plume the authors concluded that the unknown process does not lead to a net ozone production.

Beside the possibility of an unknown oxidant other factors have been discussed in literature and should be taken into consideration.

Calvert and Stockwell (1983) found that at low NO_x/CO and NO_x/hydrocarbon ratios ($<$0.05 and 0.2, respectively) artefact deviations from PSS due to rapid changes in O_3 concentration are significant. These changes can be caused by reactions other than photochemical production of ozone. Carpenter et al. (1998) discuss the loss reaction of ozone with HO_2 radicals which competes with the reaction of O_3 and NO under clean tropospheric conditions ([NO]$<$50 ppt). The strong increase in NO_2/NO (and Φ) with decreasing NO at low NO levels which is observed in our data (Fig. 6) could be explained by such processes. The ozone mixing ratios in all our data are highest at low NO_x levels and the NO_x/CO ratio is lower than 0.05 for more than 99% of all data. However, rapid changes in ozone concentrations are not observed. The question remains open to what extent these processes contribute to the observed deviations.

The use of (10) to calculate peroxy radicals implies that steady state conditions are reached and maintained at all times. However, it is possible that rapid changes of the solar flux by rapidly changing cloud cover causes some scatter or even a bias in the results of the PSS method. This question was investigated by Cantrell et al. (1993) in model calculations simulating changes in solar flux observed during the ROSE field experiment. These theoretically determined RO_2 values showed strong spikes as the solar flux increased (positive) and decreased (negative) and agreed well with PSS derived values when the solar irradiance was relatively constant for several minutes. It could be concluded from these results that variations in the solar irradiance as encountered during ROSE can introduce significant scatter in the PSS data and provide a bias towards higher PSS derived RO_2 levels. To test this effect in the MOHp data set presented here, the data were selected to include only data for which the J_{NO_2} values before and after a RO_2 measurement were higher than $0.006\,s^{-1}$. Since the situation of intermittent attenuation of the sunlight by clouds is not typical for MOHp the data selection only affects 3% of the data points. Artefact deviation due to rapid changes in the solar flux can thus be excluded for the MOHp data.

5 Conclusions

Continuous long-term measurements of NO, NO_2, O_3, J_{NO_2} over a four-year period were used to investigate photostationary state (PSS) conditions at the MOHp site and to reveal conditions which lead to deviations from PSS. The pollution

level of advected air masses is relatively low (yearly average of NO_x is below 3.5 ppb), however, maximum values can sometimes reach more than 10 ppb. In average PSS (i.e. Φ_{ext}=1±0.2) was reached in 17% (1999), 13% (2000), 22% (2001) and 32% (2002) of all cases with a strong dependence on wind direction.

A discussion of these results indicates that local conditions cause the main part of the deviations. It could be shown that Φ is strongly dependent on the height of the sampling point relative to the nearby vegetation, the horizontal distance to the forest, and the general orography determining the air flow to the station. We conclude that photolysis of NO_2 is reduced with the reduction of light penetration in the forest sub-canopy leading to increased NO_2/NO ratios due to reaction of NO with O_3 in air masses which are transported through the forest. These effects can be large enough to obscure chemical reactions, e.g. involving an unknown oxidant.

In order to analyse factors other than the local effects, PSS derived and RO_2 radicals measured during a campaign are compared for a sector for which local effects are found to be smallest. PSS derived RO_2 were systematically higher than measured ones by a factor of 2–3. Thus, other oxidation processes must be assumed to explain the observed discrepancy.

The identification of the local effect and its influence on the deviation from PSS was only possible because a relatively large data base was available from continuous long-term measurements at the site. Data from a short-term campaign could not have revealed the effects. The conditions at MOHp in terms of location and surrounding are, however, not unusual for ground stations. Other stations at which deviations from PSS are observed may have been influenced by local effects to a similar degree. The presented results make clear that the investigation of the PSS requires free advection of air masses for all wind directions and spatially homogeneous irradiance (especiall no shading by trees and buildings) in a surrounding defined by the life time of NO and NO_2 with respect to interconversions.

Acknowledgements. The authors would like to thank R. T. Wilhelm, R. Schafranek, and E. Tensing for their technical assistance. The help of B. Bohn and A. Hofzumahaus (FZ-Juelich, Germany) with calibrating our filter radiometers and discussing the accuracy of J_{NO_2} measurements is gratefully acknowledged.

Edited by: W. Sturges

References

Atkinson, R., Baulch, D. L., Cox, R. A., Crowley, J. N., Hampson Jr., R. F., Kerr, J. A., Rossi, M. J., and Troe, J.: Summary of Evaluated Kinetic and Photochemical Data for Atmospheric Chemistry, IUPAC Subcommitee on Gas Kinetic Data Evaluation for Atmospheric Chemistry, Web Version 2002.

Baumann, K., Williams, E. J., Angevine, W. M., Roberts, J. M., Norton, R. B., Frost, G. J., Fehsenfeld, F. C., Springston, S. R., Bertman, S. B., and Hartsell, B.: Ozone production and transport near Nashville, Tennessee: Results from the 1994 study at New Hendersonville, J. of Geophys. Res., Vol. 105, D7, 9137–9153, 2000.

Calvert, J. G. and Stockwell, W. R.: Deviations from the O_3-NO-NO_2 photostationary state in tropospheric chemistry, Can. J. Chem., Vol. 61, 983–992, 1983.

Cantrell, C. A., Shetter, R. E., Calvert, J. G., Parrish, D. D., Fehsenfeld, F. C., Goldan, P. D., Kuster, W., Williams, E. J., Westberg, H. H., Allwine, G., and Martin, R.: Peroxy Radicals as measured in ROSE and estimated from Photostationary State Deviations, J. of Geophys. Res., Vol. 98, D10, 18 355–18 366, 1993.

Cantrell, C. A., Shetter, R. E., Calvert, J. G., Eisele, F. L., Williams, E., Baumann, K., Brune, W. H., Stevens, P. S., and Mather, J. H.: Peroxy radicals from photostationary state deviations and steady state calculations during the Tropospheric OH Photochemistry Experiment at Idaho Hill, Colorado, 1993, J. of Geophys. Res., Vo. 102, D5, 6369–6378, 1997.

Carpenter, L. J., Clemitshaw, K. C., Burgess, R. A., Penkett, S. A., Cape, J. N., and McFaden, G. G.: Investigation and evaluation of the NO_x/O_3 Photochemical Steady State, Atmos. Environ., 32, 19, 3353–3365, 1998.

Carslaw, D. C. and Beevers, S. D.: Investigating the potential importance of primary NO_2 emissions in a street canyon, Atmos. Environ., 38, 3585–3594, 2004.

Davis, D. D., Chen, G., Chameides, W., Bradshaw, J., Sandholm, S., Rodgers, M., Schendal, J., Madronich, S., Sachse, G., Gregory, G., Anderson, B., Barrick, J., Shipham, M., Collins, J., Wade, L., and Blake, D.: A Photostationary State Analysis of the NO_2-NO System Based on Airborne Observations From the Subtropical/Tropical North and South Atlantic, J. of Geophys. Res., Vol 98, D12, 23 501–23 523, 1993.

Frost, G. J., Trainer, M., Allwine, G., Buhr, M. P., Calvert, J. G., Cantrell, C. A., Fehsenfeld, F. C., Goldan, P. D., Herwehe, J., Hübler, G., Kuster, W. C., Martin, R., McMillen, R. T., Montzka, S., A., Norton, R. B., Parrish, D. D., Ridley, B. A., Shetter, R. E., Walega, J. G., Watkins, B. A., Westberg, H. H., and Williams, E. J.: Photochemical ozone production in the rural southeastern United States during the 1990 Rural Oxidants in the Southern Environment (ROSE) program, J. of Geophys. Res., 104, D17, 22 491–22 508, 1998.

Handisides, G. M., Plass-Dülmer, C., Gilge, S., Bingemer, H., and Berresheim, H.: Hohenpeissenberg Photochemical Experiment (HOPE 2000): Measurements and photostationary state calculations of OH and peroxy radicals, Atmos. Chem. Phys., 3, 1565–1588, 2003.

Hauglustaine, D. A., Madronich, S., Ridley, B. A., Walega, J. G., Cantrell, C. A., and Shetter, R. E.: Observed and model-calculated photostationary state at Mouna Loa Observatory during MLOPEX 2, J. of Geophys. Res., Vol. 101, D9, 14 681–14 696, 1996.

Hausmann, M. and Platt, U.: Spectroscopic measurement of bromine oxide and ozone in the high Arctic during Polar Sunrise Experiment 1992, J. Geophys. Res., 99, 25 399–25 413, 1994.

Kraus, A., Rohrer, F., and Hofzumahaus, A.: Intercomparison of NO_2 photolysis frequency measurements by actinic flux spectroradiometry and chemical actinometry during JCOM97, J. Geophys. Res., 27, 1115–1118, 2000.

Leighton, P. A.: Photochemistry of Air Pollution, Academic, San Diego, California, 1961.

Merienne, M. F., Jenouvrier, A., and Coquart, B.: The NO_2 absorption spectrum: 1. Absorption cross sections at ambient temperature in the 300–500 nm region, J. Atmos. Chem., 20, 281–297, 1995.

Parrish, D. D, Trainer, M., Williams, E. J., Fahey, D. W., Hübler, G., Eubank, C. S., Liu, S. C., Murphy, P. C., Albritton, D. L., and Fehsenfeld, F. C.: Measurements of the NO_x-O_3 Photostationary State at Niwot Ridge, Colerado, J. of Geophys. Res., Vol. 91, D5, 5361–5370, 1986.

Parrish, D. D, Holloway, J. S., and Fehsenfeld, F. C.: Routine, continuous measurement of carbon monoxide with parts per billion precision, Environ. Sci. Technol., 28, 1615–1618, 1994.

Ridley, B. A., Madronich, S., Chatfiled, R. B., Walega, J. G., Shetter, R. E., Carroll, M. A., and Montzka, D. D.: Measurements and Model Simulations of the Photostationary State during the Mauna Loa Observatory Photochemistry Experiment: Implications for Radical Concentrations and Ozone Production and Loss Rates, J. of Geophys. Res., Vol. 97, D7, 10 375–10 388, 1992.

Rohrer, F., Brüning, E. S., Grobler, E. S., Weber, M., Ehhalt, D. H., Neubert, R., Schüßler, W., and Levin, I.: Mixing Ratios and Photostationary State of NO and NO_2 observed during the POPCORN Field Campaign at a Rural Site in Germany, J. Atmos. Chem., 31, 119–137, 1998.

Sander S. P., Friedl R. R., Golden D. M., Kurylo M. J., Huie R. E., Orkin V. L., Moortgat G. K., Ravishankara A. R., Kolb C. E., Molina M. J., and Finlayson-Pitts B. J.: Chemical Kinetics and Photochemical Data for Use in Atmospheric Studies, http://jpldataeval.jpl.nasa.gov/, 2003.

Schwander, H., Koepke, P., Ruggaber, A., Nakajima, T., Kaifel, A., and Oppenrieder, A.: STARSci 2.1: System for Transfer of Atmospheric Radiation, http://www.meteo.physik.uni-muenchen.de/strahlung/uvrad/Star/STARinfo.htm, 2001.

Troe, J.: Are primary quantum yields of NO_2 photolysis at $\lambda \leq 398$ nm smaller than unity? Zeit. Phys. Chem., 214, Vol. 5, 573–581, 2000.

Volz-Thomas, A., Pätz, H. W., Houben, N., Konrad, S., Mihelcic, D., Klüpfel, T., and Perner, D.: Inorganic trace gases and peroxy radicals during BERLIOZ at Pabstthum: An investigation of the photo stationary state of NO_x and O_3, J. of Geophys. Res., Vol. 108, D4 10.1029/2001JD001255, 2003.